J|A|C|S
ARTICLES
Published on Web 09/14/2006

Modular α-Helical Mimetics with Antiviral Activity against Respiratory Syncitial Virus

Nicholas E. Shepherd,[†] Huy N. Hoang,[†] Vishal S. Desai,[‡] Eric Letouze,[†] Paul R.Young,[‡] and David P. Fairlie*,[†]

Contribution from the Centre for Drug Design and Development, Institute for Molecular Bioscience University of Queensland, Brisbane, Qld 407, Australia, and School of Molecular and Microbial Science, University of Queensland, Brisbane, Qld 4072, Australia

Received June 9, 2006; E-mail: d.fairlie@imb.uq.edu.au

Abstract: A 13-residue peptide sequence from a respiratory syncitial virus fusion protein was constrained in an α-helical conformation by fusing two back-to-back cyclic α-turn mimetics. The resulting peptide, Ac−(3→7; 8→12)-bicyclo-FP[KDEFD][KSIRD]V-NH_2, was highly α-helical in water by CD and NMR spectroscopy, correctly positioning crucial binding residues (F488, I491, V493) on one face of the helix and side chain−side chain linkers on a noninteracting face of the helix. This compound displayed potent activity in both a recombinant fusion assay and an RSV antiviral assay (IC_{50} = 36 nM) and demonstrates for the first time that back-to-back modular α-helix mimetics can produce functional antagonists of important protein−protein interactions.

Introduction

α-Helical sequences of amino acids make up ∼30% of protein structure, play crucial roles in stabilizing tertiary structure, and mediate important biological processes through interactions with proteins, DNA, or RNA.[1] α-Helical recognition motifs in transcription factors, cytokines, chemokines, growth factors, GPCR-activating hormones, and RNA-transporters typically present one helical face of one to three connected α-turns for receptor binding.[1b,2] However, short peptides corresponding to these regions are not stable α-helices in water.[3] Attempts to stabilize or mimic short α-helices with unnatural amino acids, organic bridges, or nonpeptidic scaffolds have had limited success.[4] Recently, we reported the structural mimicry of a single turn of an α-helix with a five-residue macrocycle that tolerated multiple amino acid variation on one helical face and was stable to denaturation and degradation.[5] Here we join two such α-turn macrocycles back-to-back to mimic contiguous α-turns of a respiratory syncitial virus (RSV) protein that mediates fusion of viral and cell membranes, enabling virus entry into cells. We demonstrate that **1** is highly α-helical in water and has potent antifusion and antiviral activity.

RSV infection is the major cause of acute lower respiratory illness (bronchiolitis, pneumonia) in infants and young children throughout the world.[6] The entry of this virus to host cells is an essential step in the virus life cycle, with membrane fusion of the virion and host cell membrane being mediated by the RSV F glycoprotein. This viral encoded protein is displayed on the virion surface as a trimer of disulfide-linked F1/F2 heterodimers. The F1 component consists of an N-terminal fusion peptide with an adjacent α-helical heptad repeat (HR-N) and a C-terminal α-helical heptad repeat (HR-C), with an adjacent membrane-spanning region separated by an extensive intrachain disulfide bonded globular domain (Figure 1).[7] Following fusion activation, the N-terminal fusion peptide is exposed, leading to its interaction with the host cell membrane, with the adjacent HR-N helices forming a trimeric coiled coil. The subsequent dramatic reorganization of the F1 glycoprotein involves the formation of a hairpin structure that relocates the three HR-C helices around the HR-N coiled coil to form an antiparallel six-helix bundle. This reorganization brings both the virus and host cell within close proximity to facilitate fusion of their respective membranes and the release of the viral RNA genome within the host cell cytoplasm (Figure 1, path A).

A deep hydrophobic groove at the C-terminus of the HR-N coiled coil is an attractive target for antiviral drug design, and

[†] Centre for Drug Design and Development.
[‡] School of Molecular and Microbial Science.

(1) (a) Cochran, A. G. *Chem. Biol.* **2000**, *7*, R85. (b) Fairlie, D. P.; West, M. L.; Wong, A. K. *Curr. Med. Chem.* **1998**, *5*, 29−62. (c) Andrews, M. J. I.; Tabor, A. B. *Tetrahedron* **1999**, *55*, 11711−11743.
(2) Tyndall, J. D. A.; Pfieffer, B.; Abbenante, G.; Fairlie, D. P. *Chem. Rev.* **2005**, *105*, 793−826.
(3) (a) Zimm, B. H.; Bragg, J. K. *J. Chem. Phys.* **1959**, *31*, 526−535. (b) Scholtz, J. M.; Baldwin, R. L. *Annu. Rev. Biophys. Biomol. Struct.* **1992**, *21*, 95−118.
(4) (a) Bracken, C.; Guylas, J.; Taylor, J. W.; Baum, J. *J. Am. Chem. Soc.* **1994**, *116*, 6431−32. Recent examples (b) Stephens, O. M.; Kim, S.; Welch, B. D.; Hodsdon, M. E.; Kay, M. S.; Schepartz, A. *J. Am. Chem. Soc.* **2005**. *127*, 13126. (c) Wang, D.; Liao, W.; Arora, P. S. *Angew. Chem. Int. Ed.* **2005**, *44*, 6525. (d) Yin, H.; Lee, G.; Sedey, K. A.; Kutzki, O.; Park, H.; Orner, B. P.; Ernst, J. T.; Wang, H.; Sebti, S. M.; Hamilton, A. D. *J. Am. Chem. Soc.* **2005**, *127*, 10191. (e) Walensky, L. D.; Kung, A. L.; Escher, I.; Malia, T. J.; Barbuto, S.; Wright, R. D.; Wagner, G.; Verdine, G. L.; Korsmeyer, S. J. *Science*. **2004**, *305*, 1466. (f) Mills, N. L.; Daugherty, M. D.; Frankel, A. D.; Guy, R. K. *J. Am. Chem. Soc.* **2006**. *128*, 3496. See ref 5a for comprehensive list.
(5) (a) Shepherd, N. E.; Hoang, H. N.; Abbenante, G.; Fairlie, D. P. *J. Am. Chem. Soc.* **2005**, *127*, 2974−2983. (b) Shepherd, N. E.; Abbenante, G.; Fairlie, D. P. *Angew. Chem., Int. Ed.* **2004**, *43*, 2687−2690.
(6) Leader, S.; Kohlhase, K. *J. Pediatr.* **2003**. *143*, S127−132.
(7) Morton, C. J.; Cameron, R.; Lawrence, L. J.; Lin, B.; Lowe, M.; Luttick, A.; Mason, A.; McKimm-Breschkin, J.; Parker, M. W.; Ryan, J.; Smout, M.; Sullivan, J.; Tucker, S. P.; Young, P. R. *Virology* **2003**, *311*, 275−288.

10.1021/ja064058a CCC: $33.50

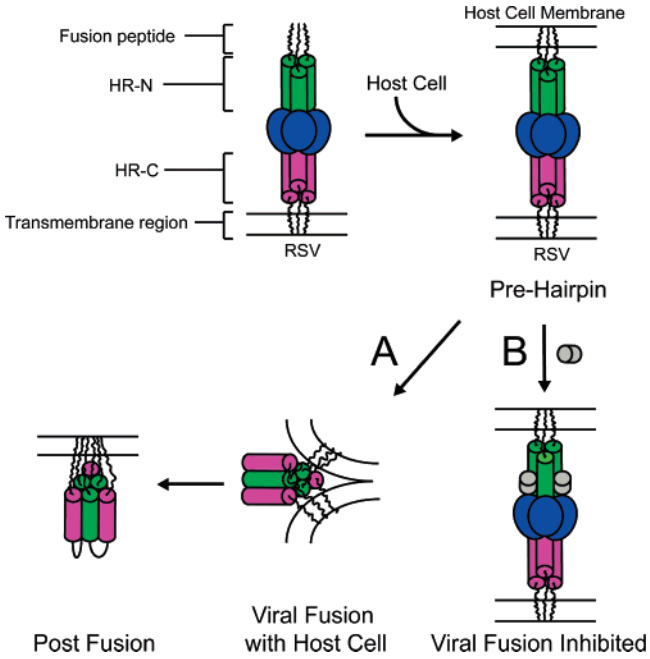

Figure 1. Structure of the F_1 glycoprotein and mechanism of viral fusion. After attaching to a host cell membrane to form the pre-hairpin, the F_1 glycoprotein can either (path A) rearrange to form a six-helix bundle that fuses the virus to the host cell membrane, the F_1 glycoprotein remaining in the postfusion state, or (path B) the HR-N trimeric coiled coil can bind to small molecules, blocking F_1 glycoprotein rearrangement and viral fusion.

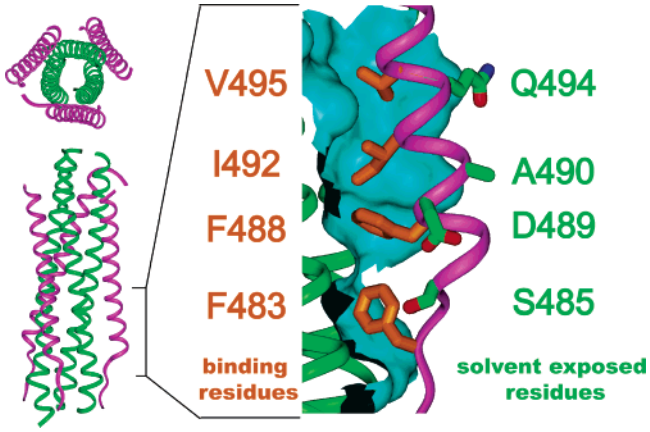

Figure 2. (Left) Top and side views of RSV fusion protein (PDB 1G2C; HR-N helices, green; HR-C helices, purple). (Right) Expansion of N-terminal region of HR-C showing residues that interact with the trimeric HR-N coiled coil (orange), and solvent exposed residues (green).

Figure 3. Designed bicyclic mimetic (**1**) of the N-terminal region of the HR-C helix from Figure 2 (binding residues in orange; solvent-exposed residues green); and corresponding linear analogue (**2**) with four alanine substitutions.

peptides and small molecules targeting this groove can potentially prevent hairpin formation, block viral fusion, and inhibit syncytia formation (Figure 1, path B).[9] A short 13-residue region of the HR-C helix, $_{483}$**F**PSDE**F**DAS**I**SQ**V**$_{495}$ (HR-C$_{483-495}$), occupies this cavity, with the major binding contributions coming from the hydrophobic residues F483, F488, I492, and V495. The presence of P484 causes a slight kink in the helix, but all residues to the C-terminus of this proline are in an α-helical conformation. Thus we sought to mimic HR-C$_{483-495}$, retaining the key helical residues (F483, F488, I492, V495) but noting that solvent-exposed S485, D489, A490, and Q494 were expendable, as they did not interact directly with the HR-N coiled coil (Figure 2, right). As a putative α-helix mimetic, we conceived **1**, Ac-cyclo-(3,7),(8,12)-**F**P[KDE**F**D][KS**I**RD]**V**-NH_2, featuring two back-to-back cyclic α-turns constrained by K(*i*)→D(*i*+4) lactam bridges (Figure 3).

Results

Synthesis of α-Helix Mimetic. Compound **1** was synthesized by Fmoc solid-phase chemistry using a resin functionalized with the Rink amide linker and a low peptide substitution loading (0.32 mmol/g) to minimize oligomer formation during cyclization. Our initial attempts to synthesize bicyclic molecules relied on an Fmoc/allyl/tBu strategy but consistently failed due to the high propensity of allyl ester protected aspartate to undergo base-induced aspartimide formation.[10] Instead, the mild acid-labile protecting groups methyltrityl (Mtt) and phenylisopropyl (Pip) were used for the bridging lysine and aspartate residues (Figure 4). In the absence of aspartimide-forming sequences, the Pip ester resembles the hindered tBu ester and provides sufficient steric bulk to prevent this deleterious side reaction. After assembling the first six residues, the lysine and aspartate side chain functionalities were deprotected with dilute TFA. Cyclization was then effected with BOP, HOAt, and excess DIPEA for in situ neutralization. Upon completion of the cyclization reaction, the procedure was then repeated to form the second macrocycle (Figure 4). Although the final isolated yield was low (10%), this method was superior to alternative orthogonal strategies (Fmoc/allyl + Hmb/tBu, Boc/Fmoc/Bn, Boc/allyl/Bn) in terms of ease, speed, purity, and rapid access to the desired bicyclic molecule. The corresponding linear analogue was also synthesized but was extremely insoluble in water and water/organic solvent mixtures, presumably due to aggregation. Linear analogue **2**, with Ala residues substituted at the solvent exposed positions, showed adequate solubility in aqueous solutions.

Structural Characterization. Circular dichroism spectra of **1** (Figure 5) showed high molar ellipticity ($[\theta]_{220}$ −25 098 deg cm^2 dmol^{-1}) and a very high $[\theta]_{220}/[\theta]_{208}$ ratio (1.07), indicative of a highly α-helical structure.[4] Under the same conditions, linear analogue **2** showed a characteristic random coil structure.

In water, **1** displayed ^{1}H NMR spectral parameters characteristic of α-helicity: low amide coupling constants (<6 Hz),[11] negative δ(Hα) shifts relative to random coil values (−0.1

(8) Zhao, X.; Singh, M.; Malashkevich, V. N.; Kim, P. S. *Proc. Natl. Acad. Sci. U.S.A.* **2000**, *97*, 14172−14177.
(9) (a) Wang, E.; Sun, X.; Qian, Y.; Zhao, L.; Tien, P.; Gao, G. F. *Biochem. Biophys. Res. Commun.* **2003**, *302*, 469−75. (b) Douglas, J. L.; Panis, M. L.; Ho, E.; Lin, K.; Krawczyk, S. H.; Grant, D. M.; Cai, R.; Swaminathan, S.; Cihlar, T. *J. Virol*. **2003**. *77*. 5054−64. (c) Cianci, C.; Yu, K.; Combrink, K.; Sin, N.; Pearce, B.; Wang, A.; Civiello, R.; Voss, S.; Luo, G.; Kadow, K.; Genovesi, E. V.; Venables, B.; Gulgeze, H.; Trehan, A.; James, J.; Lamb, L.; Medina, I.; Roach, J.; Yang, Z.; Zadjura, L.; Colonno, R.; Clark, J.; Meanwell, N.; Krystal, M. *Antimicrob. Agents Chemother*. **2004**, *48*, 413. (d) Chan, D. C.; Chutkowski, C. T.; Kim, P. S. *Proc. Natl. Acad. Sci. U.S.A.* **1998**, *95*, 15613−17. (e) Judice, K. J.; Tom, J. K.; Huang, W.; Wrin, T.; Vennari, J. Petropoulos, C. J.; McDowell, R. S. *Proc. Natl. Acad. Sci. U.S.A.* **1997**, *94*, 13426−13430.
(10) Offer, J.; Quibell, M.; Johnson, T. *J. Chem. Soc.* **1996**, *2*, 175−83.
(11) Pardi, A.; Billeter, M.; Wuthrich, K. *J. Mol. Biol*. **1984**, *180*, 741.

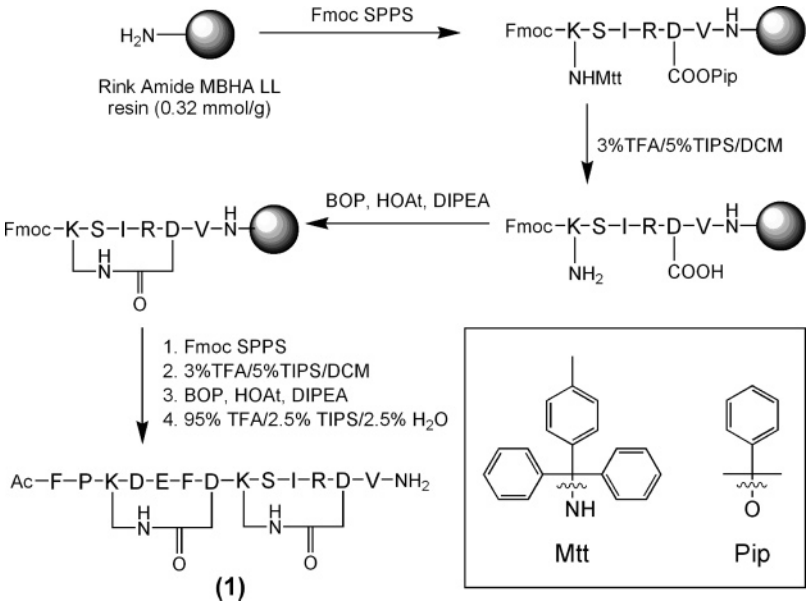

Figure 4. Strategy used to synthesize HR-C mimetic **1**. Structures of the mild acid labile protecting groups Mtt and Pip are shown boxed.

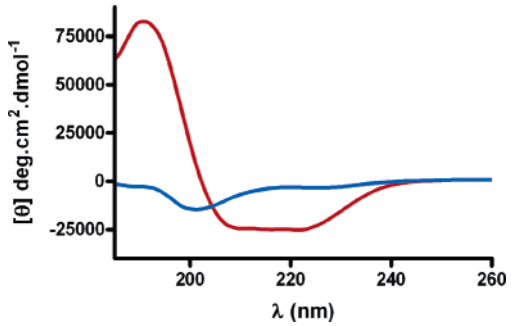

Figure 5. Circular dichroism spectra of mimetic **1** (red) and linear analogue **2** (blue) in aqueous 10 mM phosphate buffer (pH 7.4) at 25 °C.

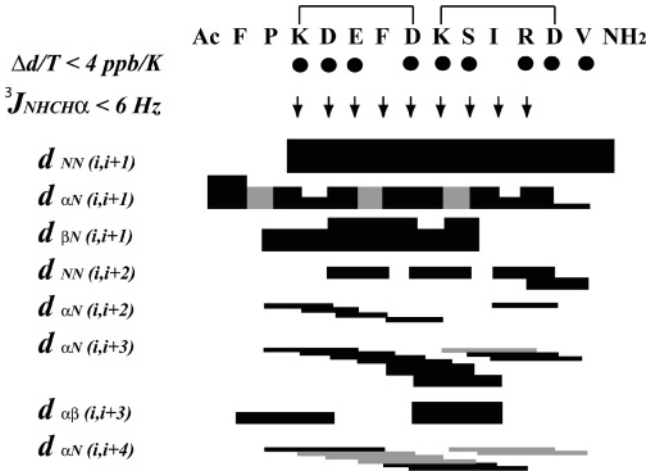

Figure 6. Summary of 1D and 2D ^{1}H NMR data for mimetic **1**. (Thickness of bars indicates the NOE intensity. Gray bars indicate overlapping signals.)

ppm),[12] low temperature dependence of amide chemical shifts (<4 ppb/K),[13] and dominant nonsequential medium-range α-helical NOEs $d_\alpha N(i,i+4)$ and $d_\alpha N(i,i+3)$ but weak 3_{10}-helical $d_\alpha N(i,i+2)$[14] (Figure 6).

A solution structure was calculated for **1** using XPLOR 3.851[15] and 72 ROE (36 sequential, 30 medium range) distance restraints and nine ϕ angle restraints. The refined 20 lowest energy structures (Figure 7, left) had no dihedral angle (>5°) or distance (>0.3 Å) violations and showed three well-defined α-helical turns between K3 and D12, with some fraying at the C-terminal V13 residue. N-terminal residues Ac−F1 and P2 displayed strong $d_{\alpha\delta}(i,i+1)$ NOEs, consistent with a *trans*-amide, but remained in an α-helical conformation. When the 20 lowest energy structures were superimposed on the structure of RSV fusion protein complex (Figure 7, right), the key residues in **1** except for the N-terminal Phe occupied the desired orientations to bind to the putative target.

Fusion Inhibition. The ability of mimetic **1** to act as an inhibitor of RSV F glycoprotein mediated fusion was assessed initially in a cell-based recombinant fusion assay. Two mammalian cell populations, HEK293 and BsrT7 cells, were cocultured after cotransfection of the HEK293 cells with pCICO.Fopt.FL (a codon-optimized full-length F gene expression plasmid driven by the CMV promoter[7]) and pGL4.80 (an expression plasmid encoding the luciferase gene under the control of the T7 promoter). Expression of the RSV F protein on the surface of the HEK293 cells mediates fusion of the two cell populations with the T7 polymerase that is constitutively expressed in the stable BsrT7 cells driving expression of the luciferase reporter gene. When a dilution series of mimetic **1** was included in the culture media at the time the cell populations were mixed, a dose−response inhibition was observed with an IC_{50} in the low nanomolar range (Figure 8). To confirm that the inhibitory effect observed was not simply due to toxicity of the compound for these cell populations, cell viability was assessed following exposure to mimetic **1**. No measurable decrease in cell viability was observed for mimetic **1** at any of the concentrations used in this study (data not shown).

Antiviral Activity. The antiviral activity of mimetic **1** was then examined in a standard infectious virus reduction assay. Cos-1 cell monolayers in microtiter plates were infected with RSV (prototype strain A2) in the presence of a dilution series

(12) Wishart, D. S.; Sykes, B. D.; Richards, F. M. *Biochemistry* **1992**, *31*, 1647.
(13) Dyson, H. J.; Cross, K. J.; Houghten, R. A.; Wilson, I. A.; Lerner, R. A. *Nature* **1985**, *318*, 480.
(14) Wüthrich, K.; Billeterm, M.; Braun, W. *J. Mol. Biol.* **1984**, *180*, 715.
(15) Brunger, A. T. Yale University: New Haven CT, 1992.

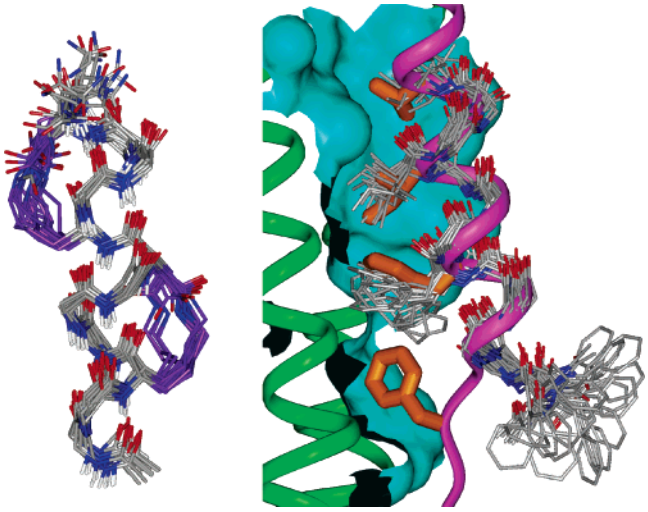

Figure 7. (Left) 20 lowest energy structures of **1** (backbone pairwise RMSD = 0.99 Å for K3−D12). (Right) 20 lowest energy structures of **1** (gray) overlayed on C-helical region of fusion protein from crystal structure (backbone, pink ribbon; protein-binding side chains, orange).

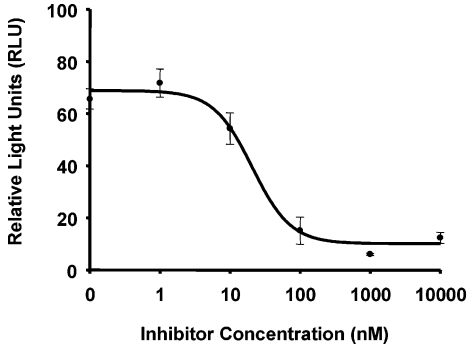

Figure 8. Cell-to-cell fusion assay of RSV F protein in the presence of mimetic **1**.

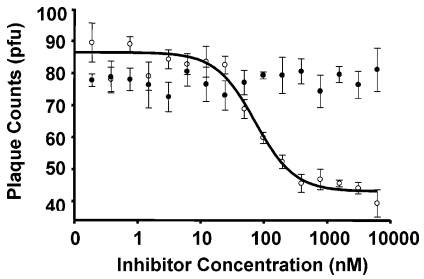

Figure 9. Antiviral activity of mimetic **1** (○), and its linear peptide equivalent **2** (●).

of either the constrained α-helical mimetic **1** or its unconstrained linear analogue **2** (Figure 9). Only mimetic **1** displayed antiviral activity, as evidenced by a reduction in RSV plaque number with an IC_{50} of 36 nM, similar to the IC_{50} of its antifusion activity and much more potent than that of the full length HR-C peptide, which only has an IC_{50} of 2.93 μM.[9] Although **1** completely inhibited fusion at higher concentrations in the recombinant fusion assay (Figure 8), complete inhibition of viral plaque formation was not observed, with an apparent resistant fraction persisting at higher concentrations. It is possible that this incomplete inhibition may represent the presence of a mixed and variably susceptible viral population or alternatively may simply reflect the dynamics of interaction of the peptide with virion displayed F protein. To date we have been unable to unambiguously distinguish between these possibilities, and such work is currently under investigation.

Discussion

This work has demonstrated a simple approach to structurally mimicking α-turns of a protein α-helix. Combinations of cyclic pentapeptide α-turn modules, each highly stable α-helices themselves,[5a] resulted here in an α-helix that both structurally and functionally mimics a biologically important region of an α-helix from within a viral fusion protein. Despite mimicking only a small fragment (13 out of 39 residues) of the viral fusion protein, **1** had potent antifusion and antiviral activity, illustrating the power of this approach to helix mimicry. The therapeutic index of the peptide is calculated to be greater than 2000, making it an attractive inhibitor for further trials.

By contrast, the corresponding unconstrained acyclic peptide sequence **2** had no α-helical structure in water and displayed no antiviral activity at or below 10 μM concentrations. The potency of **1** for inhibiting RSV fusion ($IC_{50} \sim 25$nM) also contrasts starkly with the potency for the full length HR-C peptide ($IC_{50} = 2.9$ μM) in a cell fusion assay,[9a] consistent with the literature report that the full length peptide is not very α-helical away from the helix bundle HR-N coiled coil.

Even though compound **1** had potent antiviral activity, the solution structure calculated for it revealed that a crucial residue (F483) did not orient correctly for interaction with the desired pocket in the putative receptor, and it is likely that a slight modification to this structure, that enables this side chain to also interact with the receptor, will yield compounds with even greater potency.

The high conservation of the fusion mechanism among many types of viruses (e.g. HIV, HTLV, influenza, SARS, Hendra, Nipah) and the availability of crystal structures for their corresponding fusion complexes suggest that this promising approach could be applied widely to inhibiting viral fusion. While small molecules with antiviral activity are normally identified either through extensive assay screening campaigns or by design on a target-by-target basis, the ease with which these α-helical mimetics can be designed and synthesized suggests that they could have diverse applications as biological probes and drug leads.

Methods

General. Fmoc-Asp(OPip)-OH was obtained from Bachem (Bubendorf, Switzerland). Fmoc-Lys(Mtt)-OH, other L-amino acids, Rink amide MBHA LL, and Rink amide MBHA resins were obtained from Novabiochem (Melbourne, Australia). Benzotriazol-1-yl-1,1,3,3-tetramethyluronium (HBTU) and benzotriazol-1-yloxytris(dimethylamino)-phosphonium (BOP) were obtained from Iris Biotech. Dimethylformamide, diisopropylethylamine, trifluoroacetic acid, and other reagents were of peptide synthesis grade and obtained from Auspep (Melbourne, Australia). Triisopropylsilane, dichloromethane, and diaminobenzidine (DAB) were obtained from Sigma-Aldrich (Sydney, Australia). Cos-1, HEK293, and RSV A2 were obtained from the American Type Culture Collection (Manassas, VA). Bsr/T7 cells (kindly provided by Klaus Conzelmann) were maintained in OptiMEM/3% FCS/1 mg/mL G418, and HEK293 cells were maintained in OptiMEM/3% FCS. OptiMEM, fetal calf serum (FCS), and G418 were from Invitrogen (Mount Waverley, Australia). The luciferase vector pGL4.80, Enduren substrate, and Cell-titre 96 reagent were from Promega.

Peptide Synthesis. Mimetic **1** was prepared on 0.16-mmol scale by manual stepwise solid-phase peptide synthesis using HBTU/DIPEA

activation for Fmoc chemistry[16] on Rink amide MBHA LL resin (substitution 0.32 mmol g^{-1}). Fmoc deprotections were achieved with 3 × 3 min treatments with DMF/piperidine (1:1). Four equivalents of amino acid and 4 equiv of diisopropylethylamine (DIPEA) were employed in each coupling step (15 min), except for Fmoc-Asp(OPip)-OH and Fmoc-Lys(Mtt)-OH, where only 2 equiv were coupled using HATU/HOAt/DIPEA activation. Coupling yields were monitored by quantitative ninhydrin assay[17] and double couplings were employed for yields below 99.6%. After the first Fmoc-Lys(Mtt)-OH residue was coupled, the phenylisopropyl ester of aspartic acid and the methyltrityl group of lysine were removed by treating the peptide resin with 3% TFA in DCM (2 × 30 min), after which the ninhydrin test gave an intense blue, opaque solution. Cyclization was effected on-resin using 3 equiv of BOP, 3 equiv of HOAt, and 3.5 equiv of DIPEA in 3 mL DMF/DMSO/NMP (1:1:1). The reaction was monitored by the ninhydrin test and was complete within shaking overnight. The same procedure was repeated to generate the second cycle. The peptide resin was then washed with DMF, MeOH/DCM, and DCM and dried under nitrogen with suction for 1 h. The linear peptide **2** was synthesized using the same Fmoc protocols as described above on Rink amide MBHA resin (0.67 mmol/g) on 0.15-mmol scale. Peptides were cleaved using 95% TFA, 2.5% TIPS, and 2.5% H_2O (10 mL) for 2 h. The resin was then filtered off and the solvent evaporated under a stream of nitrogen. The peptides were precipitated with cold diethyl ether. The ether was decanted to give white solids that were redissolved in 1:1 acetonitrile/water and lyophilized. The crude peptides were purified by rp-HPLC (Vydac C18 column, 300 Å, 22 × 250 mm, 214 nm; solvent A = 0.1% TFA in H_2O; solvent B = 0.1% TFA, 10% H_2O in acetonitrile; gradient 0% B to 70% B over 35 min).

Ac-FP-(cyclo-(3,7),(8,12)-[KDEFD][KSIRD]V-NH_2 (1): 35 mg (10%); [obsd ($M + H^+$) 1600.87] [calcd ($M + H^+$) 1600.77]. t_R = 21.86 min.

Ac-FPADEFAASIRAV-NH_2 (2): 50 mg (20%); [obsd ($M + H^+$) 1434.74] [calcd ($M + H^+$) 1434.59]. t_R = 20.94min.

NMR Spectroscopy. The sample for NMR analysis of mimetic **1** was prepared by dissolving the peptide (6.0 mg, 4.54 μmol) in 600 μL of H_2O and 60 μL of D_2O at pH 4.0 (pH adjusted using 0.1 M HCl or NaOH). 1D and 2D ^{1}H NMR spectra were recorded on a Bruker Avance DRX-600 spectrometer. 2D ^{1}H NMR spectra were recorded in phase-sensitive mode using time-proportional phase incrementation for quadrature detection in the t_1 dimension.[18] The 2D experiments included TOCSY (standard Bruker mlevgpph pulse program) and NOESY (standard Bruker noesygpph pulse program) and dqfCOSY (standard Bruker dqfcosygpph pulse program). TOCSY spectra were acquired over 6887 Hz with 4096 complex data points in F_2, 512 increments in F_1, and 32 scans per increment. NOESY spectra were acquired over 6887 Hz with 4096 complex data points in F_2, 512 increments in F_1, and 48 scans per increment. TOCSY and NOESY spectra were acquired with an isotropic mixing time of 80 and 300 ms, respectively. For all NMR experiments, water suppression was achieved using a modified WATERGATE sequence.[19] For 1D ^{1}H NMR spectra acquired in H_2O/D_2O (9:1), the water resonance was suppressed by low-power irradiation during the relaxation delay (1.5 s). Spectra were processed using Topspin (Bruker, Germany) software. The t_1 dimensions of all 2D spectra were zero-filled to 1024 real data points with 90° phase-shifted QSINE bell window functions applied in both dimensions followed by Fourier transformation and fifth-order polynomial baseline correction. ^{1}H NMR chemical shifts were referenced to DSS (δ 0.00 ppm) in water. $^3J_{NHCH\alpha}$ coupling constants were measured directly from 1D ^{1}H NMR.

Structure Calculation. The distance restraints used in calculating a solution structure for **1** in water were derived from NOESY spectra (recorded at 310 K) using a mixing time of 300 ms. NOE cross-peak volumes were classified manually as strong (upper distance constraint ≤2.7 Å), medium (≤3.5 Å), weak (≤5.0 Å), and very weak (≤6.0 Å), and standard pseudoatom distance corrections[5] were applied for nonstereospecifically assigned protons. To address the possibility of conformational averaging, intensities were classified conservatively and only upper distance limits were included in the calculations to allow the largest possible number of conformers to fit the experimental data. Backbone dihedral angle restraints were inferred from $^3J_{NHCH\alpha}$ coupling constants in 1D spectra at 310 K, and ϕ was restrained to $-65 \pm 30°$ for $^3J_{NHCH\alpha} \leq 6$ Hz. There was no evidence of a *cis*-amide about F1−P2 (i.e. no CHα-CHα *i*, *i*+1 NOEs) in the NOESY spectra, so all ω-angles were set to trans ($\omega = 180°$). Starting structures with randomized ϕ and ψ angles and extended side chains were generated using an ab initio simulated annealing protocol. The calculations were performed using the standard force field parameter set (PARALLHDG.PRO) and topology file (TOPALLHDG.PRO) in XPLOR with in house modifications to generated lactam bridges between lysine and aspartic acid residues. Refinement of structures was achieved using the conjugate gradient Powell alogrithm with 1000 cycles of energy minimization and a refined force field based on the program CHARMm. Structures were visualized with InsightII and analyzed for distance (>0.2 Å) and dihedral angle (>2°) violations using noe.inp and noe2emin.inp files. Final structures contained no distance violations (>0.3 Å) or angle violations (>5°).

Circular Dichroism Spectroscopy. CD measurements were performed using a Jasco model J-710 spectropolarimeter that was routinely calibrated with (1*S*)-(+)-10-camphorsulfonic acid. The peptides were dissolved in 10 mM phosphate buffer (peptide concentration 155 μM) at pH 7.1. Spectra were recorded at room temperature (298 K), with a 0.1 cm Jasco quartz cell over the wavelength range 260−185 nm at 50 nm/min with a bandwidth of 1.0 nm, response time of 2 s, resolution step width of 0.1 nm, and sensitivity of 20−50 Mdeg. Each spectrum represents the average of five scans. Spectra were analyzed using the spectral analysis software and smoothed using an "adaptive smoothing" function.

Cell Viability Assay. HEK293 cells were seeded into the wells of a 96-well microtiter plate at a confluency of ~80% and incubated at 37 °C for 48 h in the presence of a dilution series of the peptides (from 1 to 10^4 nM). Cell viability was then measured using the Cell-titre 96 reagent (Promega, Australia) as per the manufacturer's instructions and cell viability measured via absorption at 405 nm (with a background subtraction of 695 nm) on a Spectramax 100.

Fusion Assay. Subconfluent monolayers of HEK293 cells were cotransfected with pCICO.Fopt.FL (a codon-optimized full-length F gene expression plasmid driven by the CMV promoter) (Morton et al.) and pGL4.80 (an expression plasmid encoding the luciferase gene under the control of the T7 promoter) using the transfection reagent Fugene-6 (Roche; Castle Hill, Australia) with a total DNA:transfection reagent ratio of 1:3. At 4 h post-transfection, transfected HEK293 and BsrT7 (a stable cell line constitutively expressing the T7 polymerase) cells were mixed and replated into 96-well microtiter plates in the presence of a dilution series of mimetic. At 24 h, post-transfection luminescence was measured in the presence of the Enduren substrate using the TriLux MicroBeta workstation (PerkinElmer; Boston, MA).

Antiviral Assay. Cos-1 cells were maintained in OptiMEM supplemented with 3% FBS. RSV plaque assays were performed on ~90% confluent monolayers of Cos-1 cells in 96-well plates. An RSV stock solution was diluted such that a 50-μL aliquot contained approximately 80 plaque forming units (pfu). Cells were rinsed with serum-free OptiMEM and a 50-μL mixture of the diluted RSV A2 stock into which the appropriate concentration of mimetic had been diluted was used for infection. After 90 min, the mimetic/virus mixture was removed

(16) Chan, W. C.; White, P. D. *Fmoc Solid-Phase Peptide Synthesis: A Practical Approach;* Oxford University Press: New York, 2000.
(17) Sarin, V. K.; Kent, S. B. H.; Tam, J. P.; Merrifield, R. B. *Anal. Biochem.* **1981**, *117*, 147−157.
(18) Marion, D.; Wüthrich, K. *Biochem. Biophys. Res. Commun*. **1983**, *113*, 967.

and replaced with OptiMEM/2% FBS. At 48 h postinfection, cells were washed with phosphate-buffered saline (PBS) and fixed with ice-cold acetone solution (80% acetone in PBS). Immunoplaque staining was carried out by first blocking the cells for 1 h in 5% milk powder/PBS at 37°C followed by three washes of 5 min each using 0.3% Tween-20/PBS. Primary antibody (a polyclonal rabbit anti-F antisera) was applied at a 1:400 concentration in 2% milk powder/PBS and incubated at 37 °C for 1 h. The cells were then washed as described above. Secondary antibody (goat anti-rabbit peroxidize conjugate from Jackson ImmunoResearch) was added at a 1:800 concentration in 2% milk powder/PBS and incubated at 37 °C for 1 h and then washed as above. Plaque visualization was then achieved following incubation at room temperature with the peroxidase substrate DAB.

Acknowledgment. We thank the Australian Research Council and the National Health & Medical Research Council for partial financial support.

Supporting Information Available: ^{1}H NMR resonances, spectral assignments, VT-NMR data, and NOE structural constraints. This material is available free of charge via the Internet at http://pubs.acs.org.

JA064058A